JMEPEG (2012) 21:1504–1508
DOI: 10.1007/s11665-011-0057-3

1059-9495/$19.00

Effect of Scandium on Microstructure and Mechanical Properties of Cast Al-Si-Mg Alloy

M.S. Kaiser, M.R. Basher, and A.S.W. Kurny

(Submitted January 23, 2011; in revised form September 6, 2011)

Microstructural modification and grain refinement due to addition of scandium in Al-6Si-0.3Mg alloy has been studied in this article. It is seen from the microstructure that the dendrites of the cast Al-6Si-0.3Mg alloy have been refined significantly because of addition of scandium. Increasing amount of scandium leads to a greater dendrite refinement. The age hardening effect has been studied by subjecting the alloys containing varying amounts of scandium ranging from 0.2 to 0.6 wt.% to isochronal and isothermal aging at various temperatures for different times. It is observed that addition of scandium is the most effective in suppressing the softening effect during prolonged aging treatment.

Keywords age hardening, Al-Si-Mg alloys, grain-refinement, precipitates, recrystallization

1. Introduction

Scandium is an effective grain refiner and increases the recrystallization temperature in aluminum alloys (Ref 1, 2). A good number of studies regarding the use of scandium in Al alloys have been reported (Ref 3-6). The use of scandium in Al alloys is meant for taking the advantage of the unique precipitation hardening behavior on the part of scandium. Scandium forms a stable LI_2 phase, Al_3Sc with aluminum. The precipitation of Al_3Sc is coherent with the matrix (Ref 6, 7). The presence of fine coherent precipitates of Al_3Sc impedes the migration of dislocations and increases the recovery temperature by stabilizing the substructures. The kinetics of recrystallization is also retarded by scandium addition (Ref 1, 3). Scandium does not form any second-phase intermetallic compound with other alloying elements, such as iron, manganese, and chromium (Ref 3). The alloy is normally used in as-cast condition and will undergo softening during use at higher temperature. However, the softening behavior of the alloy system under the influence of Al_3Sc particles preexisting in the matrix has not been studied elaborately. This article discusses the results of investigations on the effects of scandium on the grain refining, aging, precipitation, and recrystallization behavior of Al-6Si-0.3Mg alloys.

2. Experimental

Four alloys were produced by melting required amounts of (i) pure aluminum (98.5% purity), (ii) piston head of Toyota car engine (11.2% Si with a small amount of magnesium and other trace elements), and (iii) aluminum-scandium master alloy (2% Sc). Melting was performed in a clay-graphite crucible in a natural gas-fired pit furnace under suitable flux cover (degasser, borax etc.). In all cases, the final temperature of the melt was maintained at 760 ± 15 °C with the help of an electronic temperature controller. Before casting, the melt was homogenized by stirring at 700 °C. Casting was done in cast iron moulds [20.0 mm in diameter x 200.0 mm in length] preheated to 200 °C. All the alloys were analyzed by wet chemical and spectrochemical methods simultaneously. The chemical compositions of the alloys are given in Table 1.

The cast alloys were cut to pieces of suitable size [16.0 mm diameter x 10.0 mm length]. Scanning electron microscopy of the cast samples was carried out by a Jeol Scanning Electron Microscope, JSM-5200. The samples in the as-cast condition were subjected to isochronal aging for 60 min at different temperatures up to 500 °C, and isothermal aging at various temperatures up to 300 °C for different periods of time ranging from 30 to 240 min. The age hardening behavior was followed by hardness measurements. A Rockwell F scale [60 kg load, and 1/16″ steel ball indenter] was used, and an average of ten concordant readings was taken as the representative hardness of a sample. In nanoindentation study, small loads and Berkovich tip with a three-sided pyramid geometry were used. The alloys, in the form of lumps of 10-15 mg in weight, have also been subjected to DSC using a Du Pont 900 instrument. Inert N_2 gas atmosphere was used, and the DSC scan was conducted over a temperature range from 50 to 550 °C. A fixed heating rate of 10°/min was used in all the scans.

3. Results

3.1 Scanning Electron Microscopy

Figure 1(a) reveals the SEM micrographs of the base alloy (Alloy 1) in as-cast condition. The Si-rich phase appeared in the micrograph as the bright constituent with the elongated plate-like morphology formed in the inter-dendritic regions.

M.S. Kaiser, Directorate of Advisory, Extension and Research Services, Bangladesh University of Engineering and Technology, Dhaka 1000, Bangladesh; **M.R. Basher** and **A.S.W. Kurny**, Department of Materials and Metallurgical Engineering, Bangladesh University of Engineering and Technology, Dhaka 1000, Bangladesh. Contact e-mail: aswkurny@mme.buet.ac.bd.

Figure 1(b) shows the SEM micrograph of 0.2 wt.% Sc containing Alloy 2. The micrographs reveal a mixed dendritic and equiaxed morphology. Figure 1(c) shows the SEM micrograph of the 0.4 wt.% Sc containing Alloy 3. It reveals that the dendritic feature of the microstructure is much reduced with increasing volume fraction of the grains having the equiaxed morphology. Comparison of Fig. 1(b) and Fig. 1(c) reveals much reduced concentration of plate-like precipitate with faceted and smooth surface. Figure 1(d), SEM micrographs of Alloy 4, reveals that the dendritic morphology is almost absent in the microstructure. The microstructure consists almost equiaxed Al grains which precipitate along the grain boundaries. It shows almost total absence of faceted plate-like particles.

3.2 Aging

Figure 2 shows the isochronal aging behavior of the different alloys. For all the alloys, the peak aging condition was attained at 250 °C. Although hardness of the base alloy was lower than the Sc-bearing alloys in the as-cast condition, the softening effect above 250 °C was found to be much more prominent in the base alloy than in the Sc-containing alloys. Figures 3-5 show the isothermal aging behavior of different alloys at different levels of temperature. At 200 °C, the base alloy attains the peak condition after 30 min. In the case of Sc-bearing alloys the peak hardness is maintained without any appreciable softening through the duration of aging. For aging in the temperature range 250-300 °C the peak aging condition

Table 1 Chemical composition of the experimental alloys (wt.%)

Alloy	Si	Mg	Sc	Pb	Ti	Cu	Fe	Mn	Ni	Zn	Cr	Sn	Al
1	5.73	0.282	0.000	0.006	0.020	0.765	0.406	0.074	0.402	0.043	0.011	0.027	Bal
2	5.57	0.305	0.180	0.007	0.025	0.838	0.404	0.069	0.404	0.040	0.011	0.029	Bal
3	5.87	0.291	0.360	0.007	0.027	0.839	0.459	0.080	0.454	0.044	0.012	0.027	Bal
4	5.88	0.289	0.550	0.008	0.034	0.875	0.409	0.077	0.393	0.039	0.012	0.026	Bal

Remarks: Alloy 1: Al-6 wt.% Si-0.3 wt.% Mg; Alloy 2: Al-6 wt.% Si-0.3 wt.% Mg-0.2 wt.% Sc; Alloy 3: Al-6 wt.% Si-0.3 wt.% Mg-0.4 wt.% Sc; Alloy 4: Al-6 wt.% Si-0.3 wt.% Mg-0.6 wt.% Sc

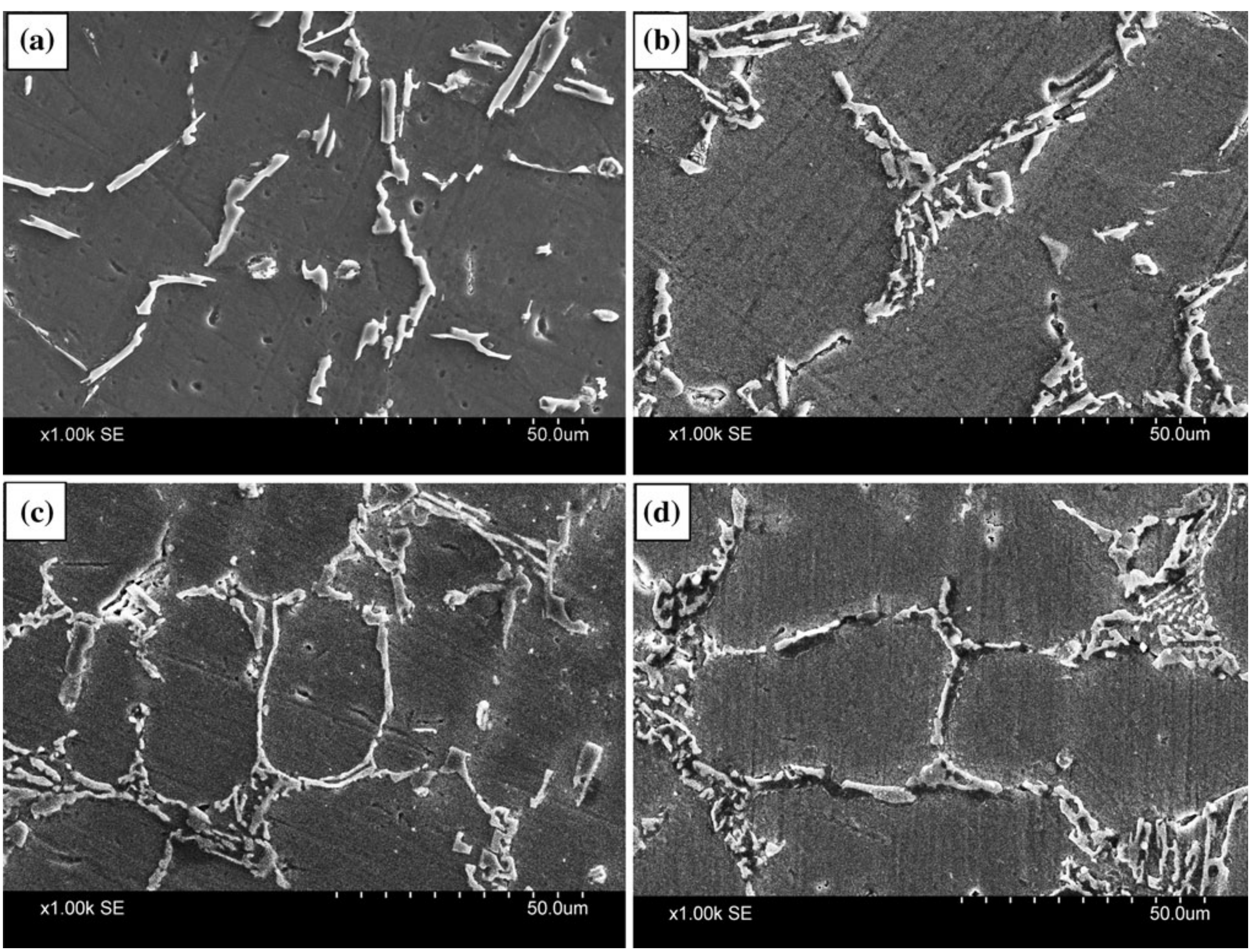

Fig. 1 SEM micrographs of the cast alloys: (a) Alloy 1; (b) Alloy 2; (c) Alloy 3; and (d) Alloy 4

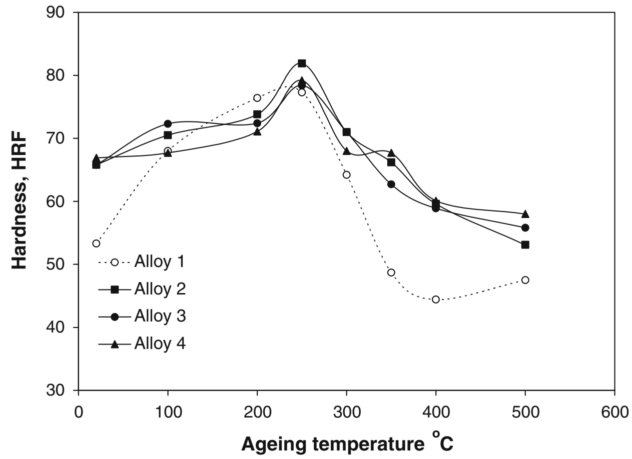

Fig. 2 Isochronal aging curve of the cast alloys, aged for 1 h

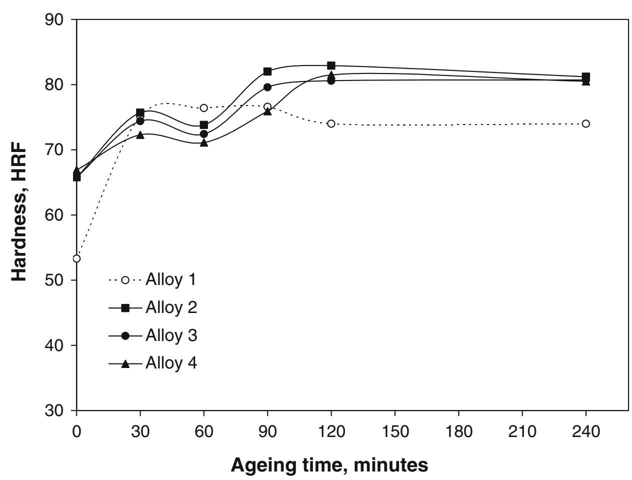

Fig. 3 Isothermal aging curve of the cast alloys, aged at 200 °C

for the base alloy was attained in 30 min. The decrease in hardness became more pronounced with increasing aging temperature in the range 250-300 °C. However, the Sc-bearing alloy exhibits stronger resistance to softening in comparison with the base alloy.

Figure 6(a)-(c) show the nanoindentation load-depth profile for the base alloy taken from the interior of grains, matrix close to the precipitates at the grain boundary, and the Si-rich phase at the grain boundary, respectively. Figure 6(d)-(f) show the similar results for the same sample after aging at 250 °C for 60 min. Comparison of Fig. 6(a)-(f) reveals that in the case of as-cast sample hardness values at different regions is higher than those for the aged samples.

Figure 7(a)-(c) show the nanoindentation load depth profile for the 0.2 wt.% scandium added Alloy 2 taken from the interior of grains, matrix close to the precipitates at the grain boundary, and the Si-rich phase at the grain boundary, respectively. Figure 7(d)-(f) show the similar results for the same sample after aging at 250 °C for 60 min. Comparison of Fig. 7(a)-(f) reveals no perceptible variation of hardness values obtained from the interior of the grain and from the matrix near the grain boundary for the cast and aged samples.

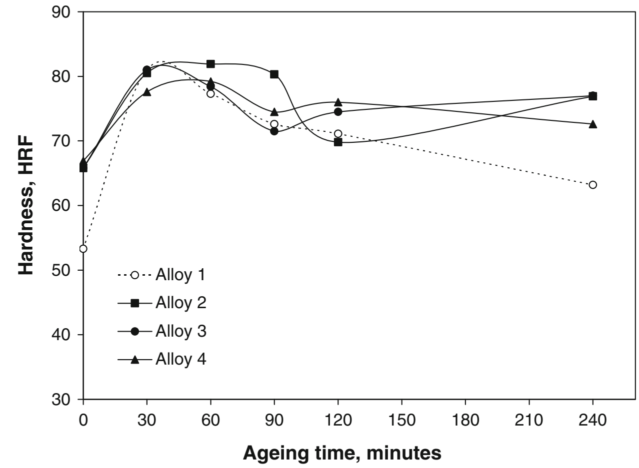

Fig. 4 Isothermal aging curve of the cast alloys, aged at 250 °C

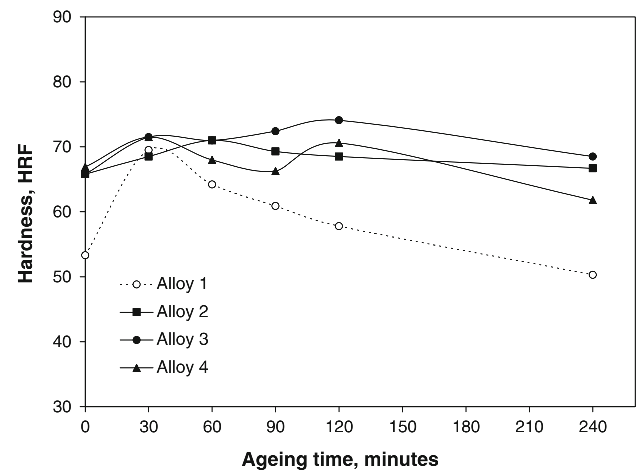

Fig. 5 Isothermal aging curve of the cast alloys, aged at 300 °C

3.3 Differential Scanning Calorimetry (DSC)

The DSC curve for the base Al-6Si-0.3Mg alloy (Fig. 8) showed a broad exothermic at 220 °C. This has been attributed to the dissolution of some phase already present in the cast alloy (Ref 8). This is followed by another exothermic peak at 460 °C. The exothermic at 460 °C corresponds to recrystallization. The DSC heating curve of alloy containing 0.2 wt.% Sc is shown in Fig. 9. An exothermic at 225 °C corresponds to the dissolution of some second-phase particle, presumably β-phase, present in the microstructure. Following this, a broad exothermic peak is seen to appear at 475 °C in the heating curve. This indicates that the recrystallization takes place at a higher temperature.

4. Discussion

Observations under optical microscopes have not provided much information; nevertheless, the overall appearance of the microstructure resembles what are normally observed in cast aluminum alloy ingot (Ref 9). The dendrites of the cast Alloy 1 are seen to have refined significantly with the addition of scandium. Reportedly (Ref 3), alloy with 0.2 wt.% Sc does not

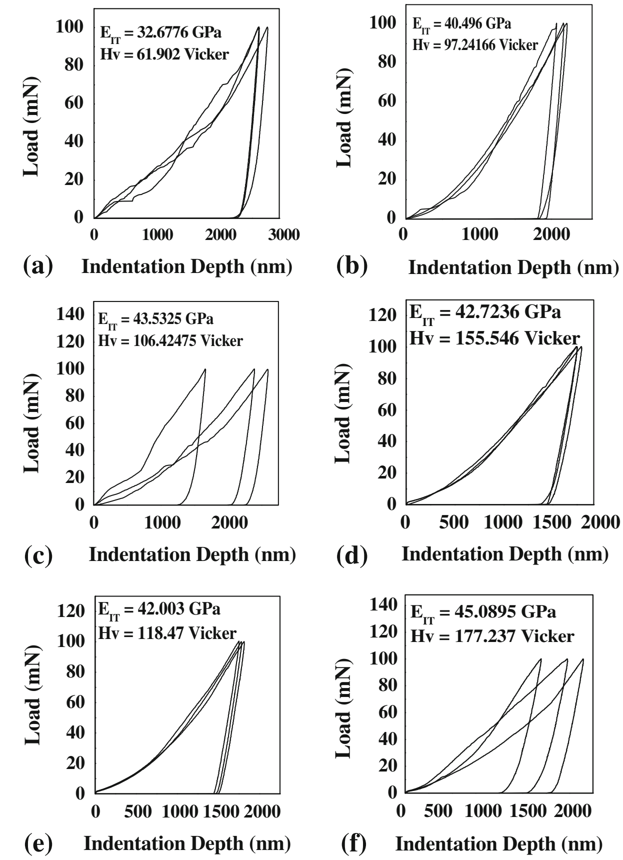

Fig. 6 Nanoindentation load-depth profile for the Alloy 1

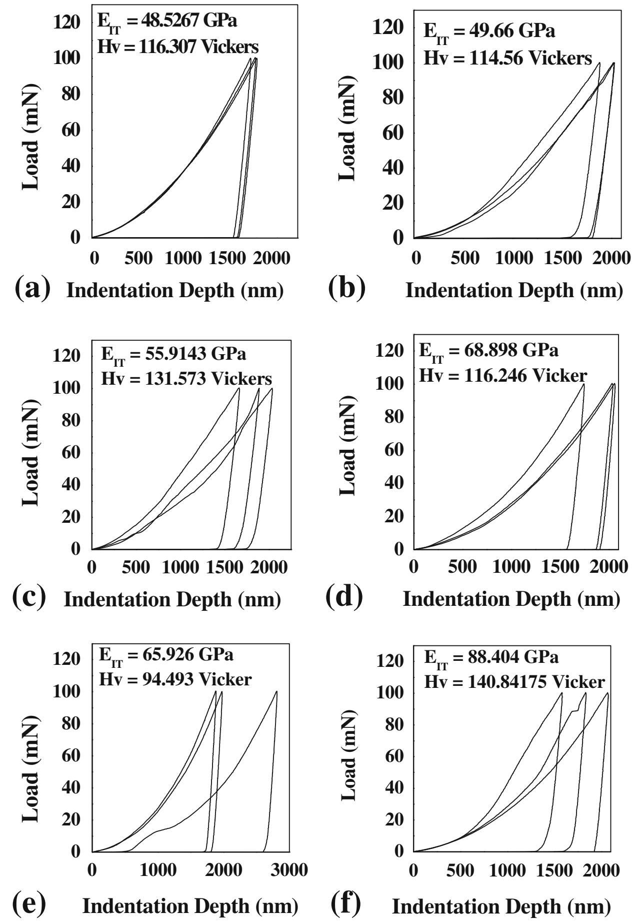

Fig. 7 Nanoindentation load-depth profile for the Alloy 2

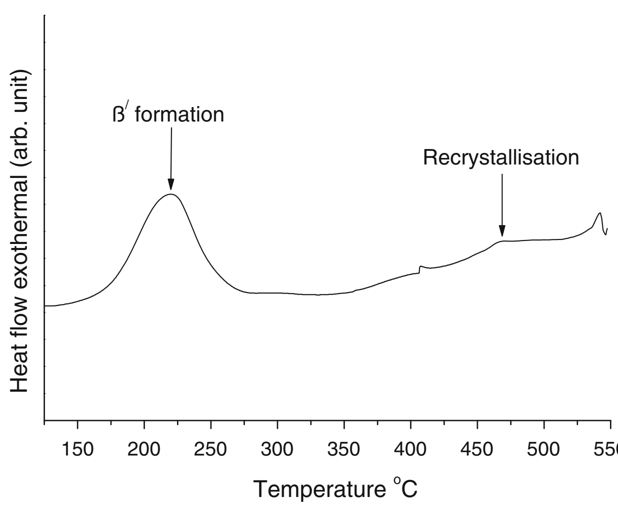

Fig. 8 DSC heating curve of cast Alloy 1

provide much grain refinement, but refines the primary dendrites of α with consequent diminution of dendrite arm spacing. The arm spacing in scandium-treated alloys were found to lie within a range of 20-40 μm against a value of around 45 μm in case of base alloy. This has been ascribed (Ref 1) to the modification of solidification speed by scandium during the growth of the dendrite structure. Also scandium-containing alloys are seen to contain less amount of intermetallic compounds. Owing to increase in solidification speed, the super-cooling effect is weakened. The consequential faster solidification leads to decrement in the amount and size of the second-phase constituents with scandium addition. The faster solidification also aids in the retention of more solute in solution. Since dendrites are refined with scandium addition, the size of individual second-phase region becomes smaller as these phases are formed within the interdendritic spaces. Increasing amount of scandium leads to a greater increase in solidification speed, and hence the related effects on dendrite refinement, and fraction, and number density of second-phase constituents have been realized more as evidenced in the microstructures of Alloys 2-4.

In isochronal aging for 1 h, maximum hardness was found at 250 °C for all alloys. The peak hardness of Alloy 1 falls more quickly than the other alloys. This is because, with the increase of temperature, Alloy 1 starts to recrystallize. However, owing to the formation of Al_3Sc, recrystallization is delayed in Alloys 2-4. This is also because of formation of Al_3Sc which results in finer grains and increase of hardness. On aging at 200 °C, hardening peak was found in 90 min. This is also because of formation of β′ (Ref 3). Again, hardness of Alloy 1 falls quicker than the other alloys because of early recrystallization. When alloys are aged at 250 °C, maximum hardness was found in 30 min. β′ is formed in less time because of higher temperature. The effect of Al_3Sc formation is clearly seen at the right portion of Fig. 4 (where the hardness of Alloy 1 decreases because of recrystallization). Aging at 300 °C gives maximum hardness in 30 min. However, this maximum hardness is less than the previous maximums. Because at

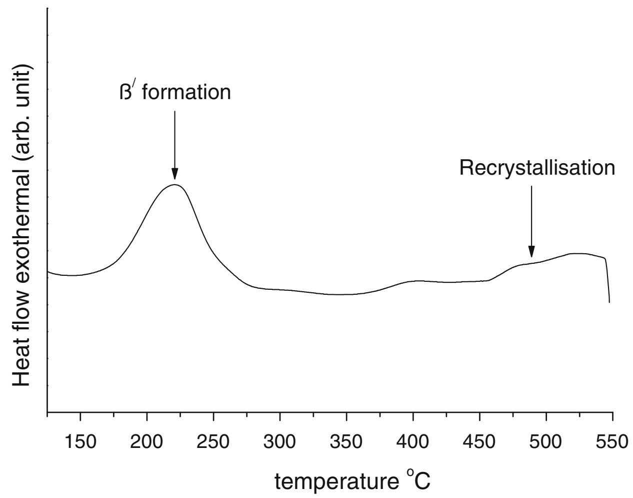

Fig. 9 DSC heating curve of cast Alloy 2

higher temperature, the precipitates tend to become coarser, and coarse precipitates are not as effective as finely dispersed precipitates to resist the movement of dislocation. Coarse precipitates also do not offer enough resistance to the recrystallization.

Comparison of Fig. 6(a)-(f) reveals that in the case of as-cast sample, hardness values at different regions are higher than those for the aged samples. This is due to precipitation of excess solute in the form of much finer precipitates or solute clusters which have not appeared in the SEM micrographs. Therefore, the results suggest that increase in bulk hardness during aging is not only due to formation of excess precipitates in the grain boundary, but also due to formation of much finer precipitates in the matrix as well as at the grain boundary. It has also been recorded that the matrix near the grain boundary yielded the lowest hardness in both the cast and aged samples. This may be attributed to the formation of larger amount of precipitates in the grain boundary regions and corresponding depletion of the solute elements in near grain boundary locations. Comparison of Fig. 7(a)-(f) reveals no perceptible variation of hardness values obtained from the interior of the grain and from the matrix near the grain boundary for cast and aged samples. This may be attributed to the fact that early precipitation of Sc has provided the nucleation sites for the Si-rich phases during later stage of solidification which brings in complete precipitation of the Si-rich phase during solidification. Certain amount of improvement in hardness has been achieved after aging for the precipitate phases at the grain boundary probably because of precipitation of Sc along with Si-rich phases. It is interesting to note that while Sc addition has improved the hardness in as-cast condition for different locations in the case of aged samples, Sc addition has lowered the hardness value.

Alloy 1 contains some metastable phase. It is reported that metastable β′ phase in Al-Si-Mg alloy gives way to the formation of β-phase (Ref 10, 11). Two separate DSC peaks noted for the alloy is suggestive of the probable dissolution of β′ phase for subsequent formation of β-phase at 220 °C. The exothermic that follows occurs at 460 °C. Recrystallization temperature is found similar to what has been reported earlier (Ref 3, 8). DSC plot of cast Alloy 2 is almost similar to cast Alloy 1. An exothermic peak denoting the formation of metastable β′ is noticed at 225 °C because the presence of dislocations might have induced the formation of a metastable phase in higher scandium alloy. This implies that with the greater volume fraction of finely distributed Al_3Sc precipitates, the dislocation movement is restricted. Hence, sub-structural stability is increased. Recrystallization takes place at a high temperature, viz., 475 °C, although it is reported that the favorable temperature for recrystallization is 400 °C. Thus, kinetics of recrystallization is greatly delayed in Al-6Si-0.3Mg-0.2Sc alloy. This is so, because the fine coherent precipitates of Al_3Sc have high coherency strains. This severely impedes the migration of dislocations. This may be due to misfit dislocations which are partially annihilated only at high temperatures after sufficient degree of particle coarsening (Ref 12).

5. Conclusion

1. The dendrites of the cast base alloy are refined significantly with the addition of scandium. Increasing amount of scandium leads to a greater dendrite refinement, and a fraction of second-phase constituents is reduced.
2. Sc addition is effective in respect of improving the hardness during aging. However, Sc addition is the most effective in suppressing the softening effect during prolonged aging treatment.
3. The precipitates delay the recrystallization in scandium-bearing alloys. The higher the volume fraction of precipitates, the higher the recrystallization start temperature becomes.

References

1. M.S. Kaiser, S. Datta, A. Roychowdhury, and M.K. Banerjee, Effect of Scandium on the Microstructure and Ageing Behaviour of Cast Al-6Mg Alloy, *Mater. Charact.*, 2008, **59**, p 1661–1666
2. S. Lathabai and P.G. Lloyd, The Effect of Scandium on the Microstructure, Mechanical Properties and Weldability of a Cast Al-Mg Alloy, *Acta Mater.*, 2002, **50**, p 4275–4292
3. L.S. Toropova, D.G. Eskin, M.L. Kharakterova, and T.V. Dobatkina, *Advanced Aluminum Alloys Containing Scandium, Structure and Properties*, Baikov Institute of Metallurgy, Moscow, 1998
4. R.R. Sawtell and C.L. Jensen, Mechanical Properties and Microstructures of Al-Mg-Sc Alloys, *Metall. Trans. A*, 1990, **21A**, p 421–430
5. M.S. Kaiser and M.K. Banerjee, Effect of Scandium on Cast Al-6Mg Alloys, *Indian Foundry J.*, 2006, **52**(8), p 29–43
6. J. Royset and N. Ryum, Scandium in Aluminium Alloys, *Int. Mater. Rev.*, 2005, **50**(1), p 19–44
7. M.E. Drits, S.G. Pavlenko, and L.S. Toropova, Mechanism of the Influence of Scandium in Increasing the Strength and Thermal Stability of Alloys in the Al-Mg System, *Sov. Phys. Dokl.*, 1981, **26**(3), p 344–346
8. S. Nagasaki and A. Maesono, High Temp. High Press, *Met. Phys.*, 1965, **11**, p 182
9. R.R. Sawtell and C.L. Jensen, Mechanical Properties and Microstructures of Al-Mg-Sc Alloys, *Metall. Trans.*, 1990, **21A**, p 421–430
10. I.J. Polmear, *Light Alloys, Metallurgy of the Light Metals*, Edward Arnold (Publishers) Ltd, London, 1981
11. Q.G. Wang and C.J. Davidson, Solidification and Precipitation Behaviour of Al-Si-Mg Casting Alloys, *J. Mater. Sci.*, 2001, **36**(1), p 739–750
12. M.S. Kaiser, P.M.G. Nambissan, M.K. Banerjee, A. Sachdeva, and P.K. Pujari, Positron Lifetime Studies and Coincidence Doppler Broadening Spectroscopy of $Al_{94-x}Mg_6Sc_x$ (x = 0 to 0.6) Alloy, *J. Mater. Sci.*, 2007, **42**(8), p 2618–2629